Electronic Supplementary Material (ESI) for Journal of Materials Chemistry A.

Supporting Information

A smart flexible supercapacitor enabled by a transparent electrochromic electrode composed of $W_{18}O_{49}$ nanowires/rGO composite films

Muhammad Hassan [a], Ghulam Abbas [a], Yao Lu [b], Ziya Wang*[a,c], Zhengchun Peng*[a]

a. Center for Stretchable Electronics and NanoSensors, Key Laboratory of Optoelectronic Devices and Systems of Ministry of Education and Guangdong Province, College of Physics and Optoelectronic Engineering, Shenzhen University, Shenzhen 518060, China

b. State Key Laboratory of Automotive Safety and Energy, Tsinghua University, Beijing 100084, China

c. Shenzhen Institute of Artificial Intelligence and Robotics for Society (AIRS), Shenzhen 518129, China

Email: zcpeng@szu.edu.cn

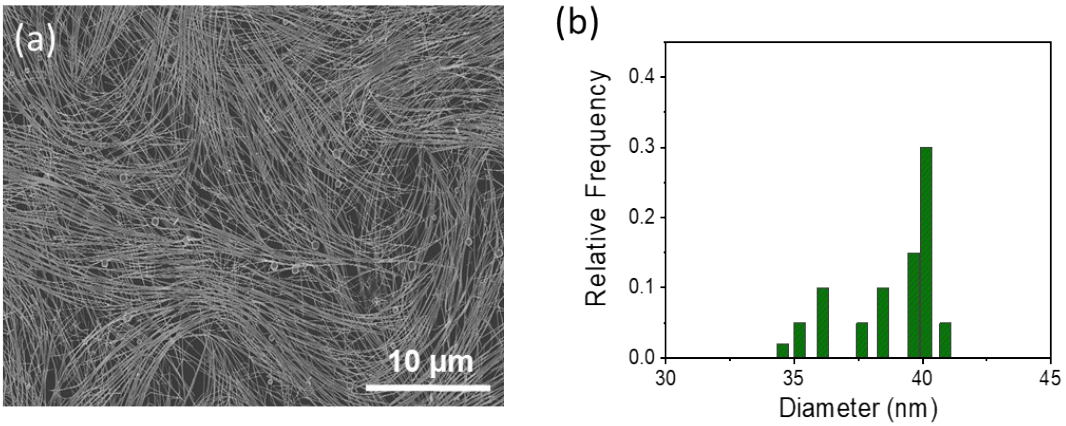

Fig. S1. (a,b) SEM image and relative frequency of Ag NWs diameter.

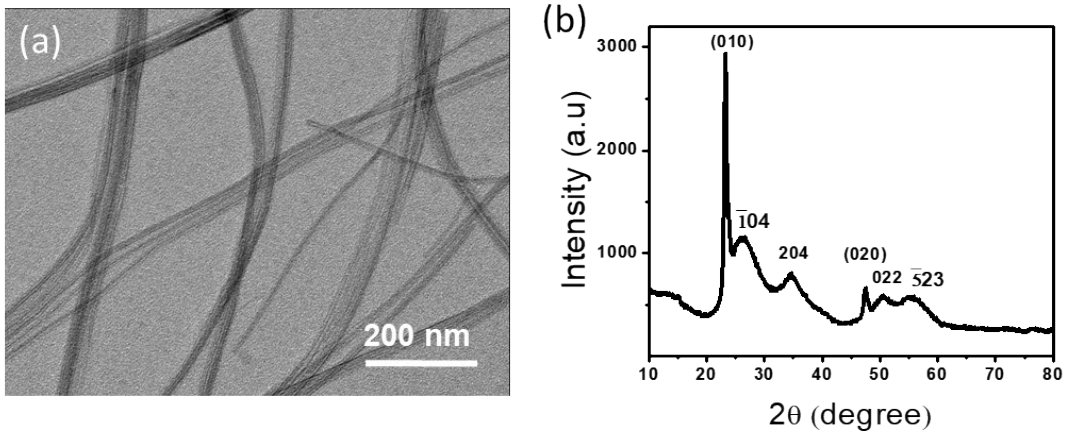

Fig. S2. (a,b) TEM image and XRD spectrum of $W_{18}O_{49}$ NWs.

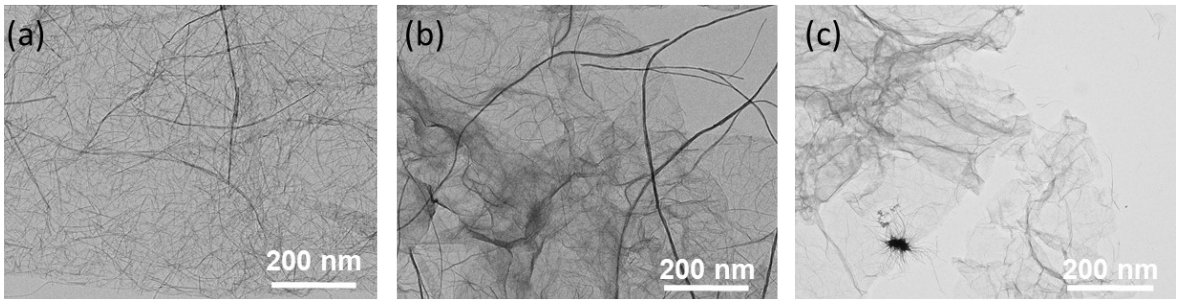

Fig. S3. TEM images of $W_{18}O_{49}$ NWs/rGO composite with different weight ratio of (a) 2 wt.%, (b) 8 wt.% and (c) 16 wt.%.

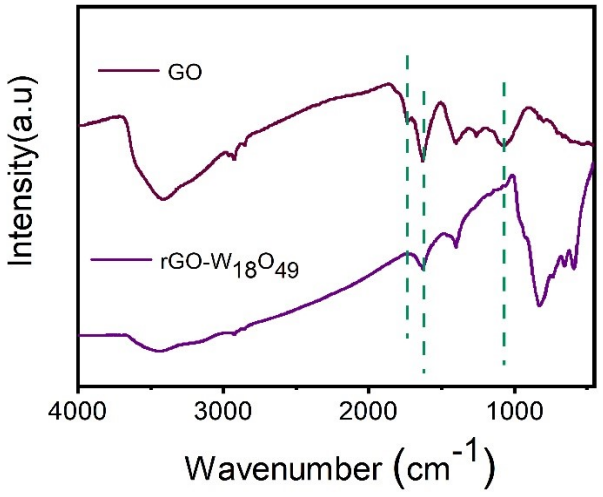

Fig. S4. IR spectrum of GO and $W_{18}O_{49}$ NWs/rGO composite.

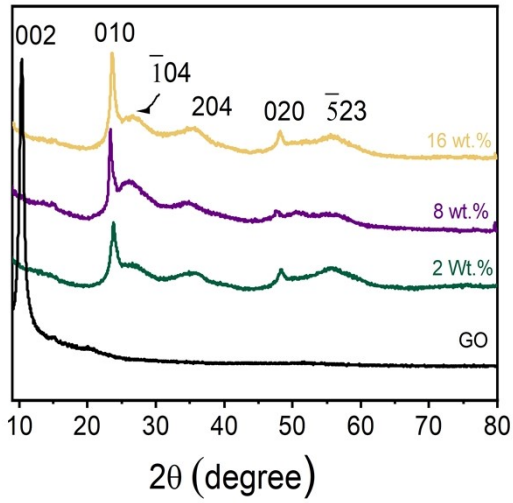

Fig. S5. XRD spectrum of pure GO and $W_{18}O_{49}$ NWs/rGO composite with weight ratio of 2 wt.%, 8 wt.% and 16 wt.%.

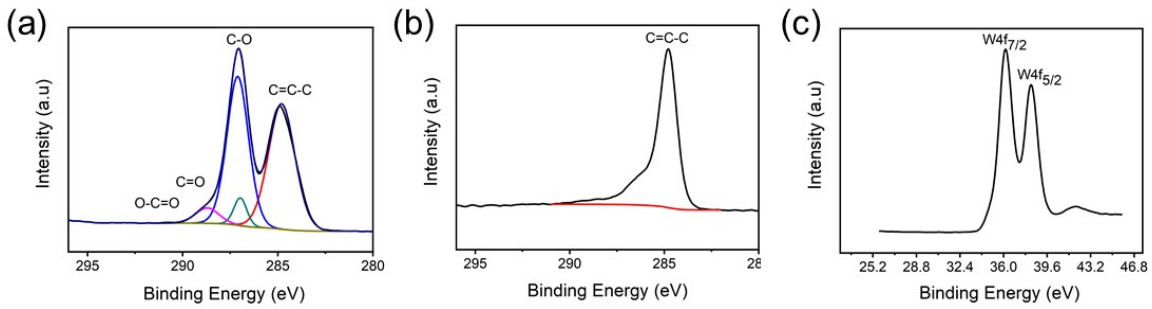

Fig. S6. (a, b, c) XPS spectra of GO and $W_{18}O_{49}$ NWs/rGO composite.

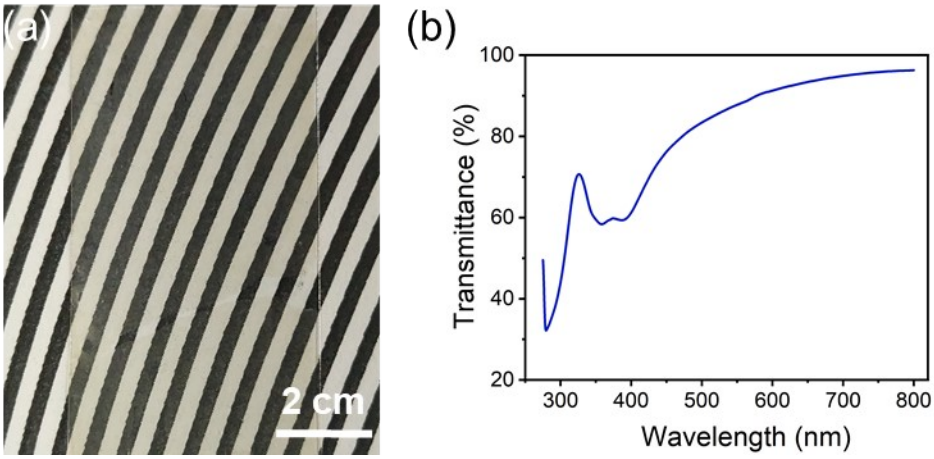

Fig. S7. (a) Photograph of flexible transparent electrode, fabricated by co-assembly of Ag and $W_{18}O_{49}$ NWs. (b) Related transmittance spectrum of film.

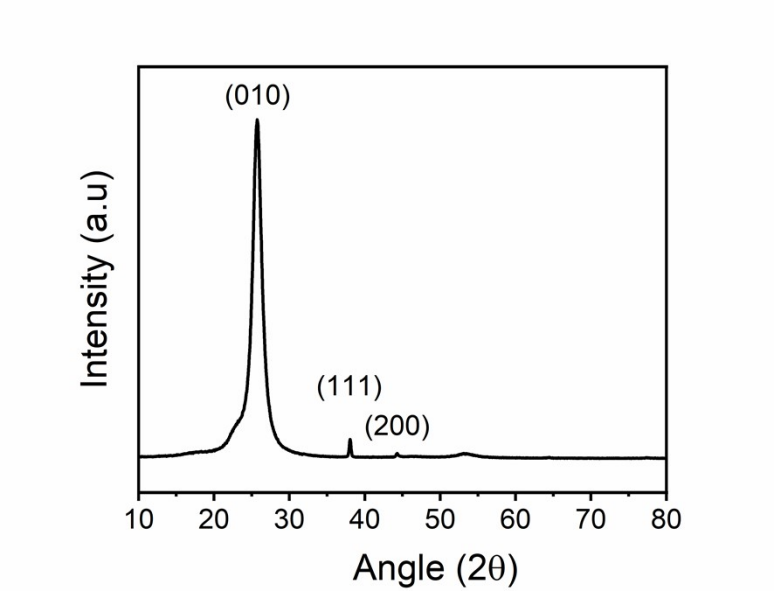

Fig. S8. XRD of $Ag/W_{18}O_{49}$ NW networks electrode.

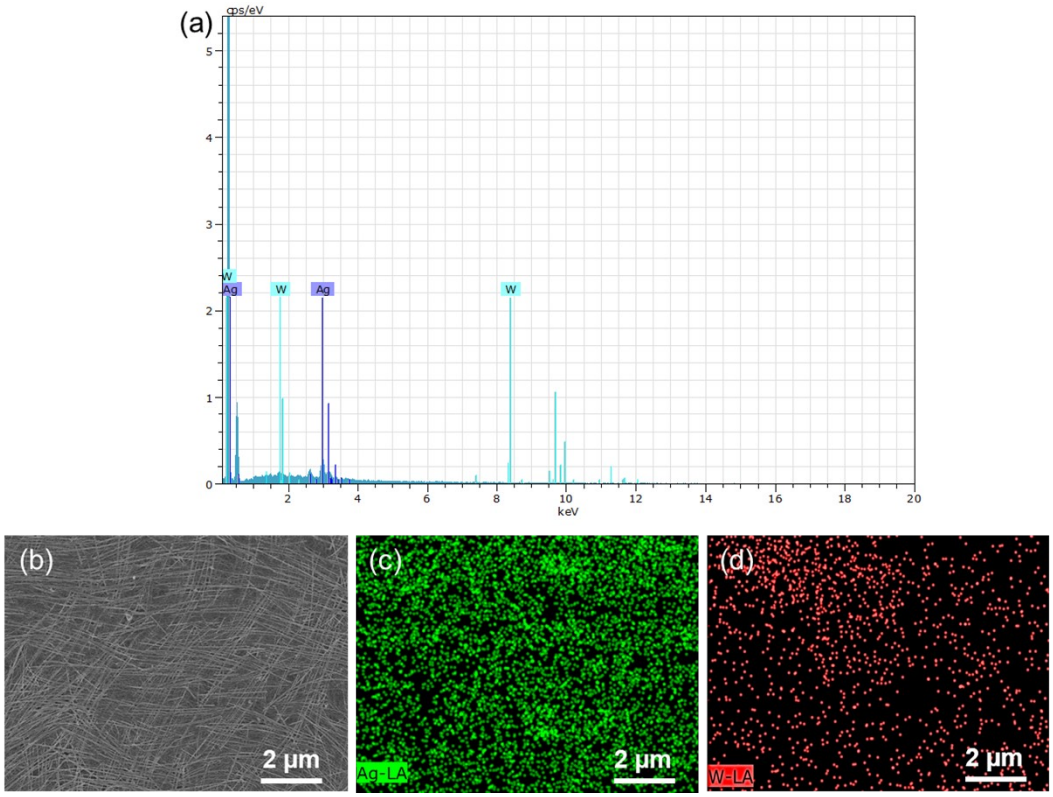

Fig. S9. EDS of $Ag/W_{18}O_{49}$ NW networks electrode. (a) EDS spectrum, (b) SEM and (c,d) EDS mapping of $Ag/W_{18}O_{49}$ NW networks electrode.

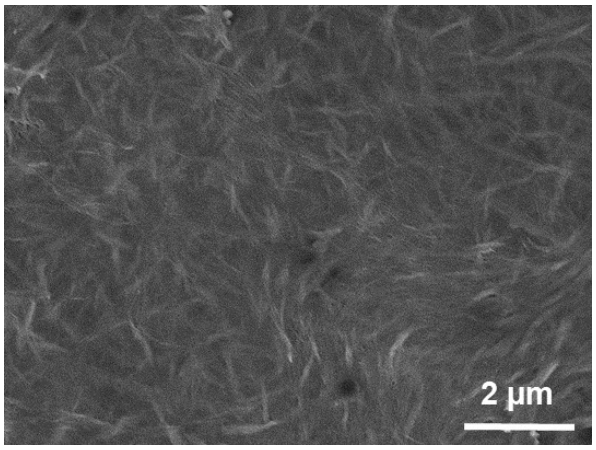

Fig. S10. SEM image of 15 layers of 8wt.% $W_{18}O_{49}$ NW/rGO composite assembled on the Ag/$W_{18}O_{49}$ NW films.

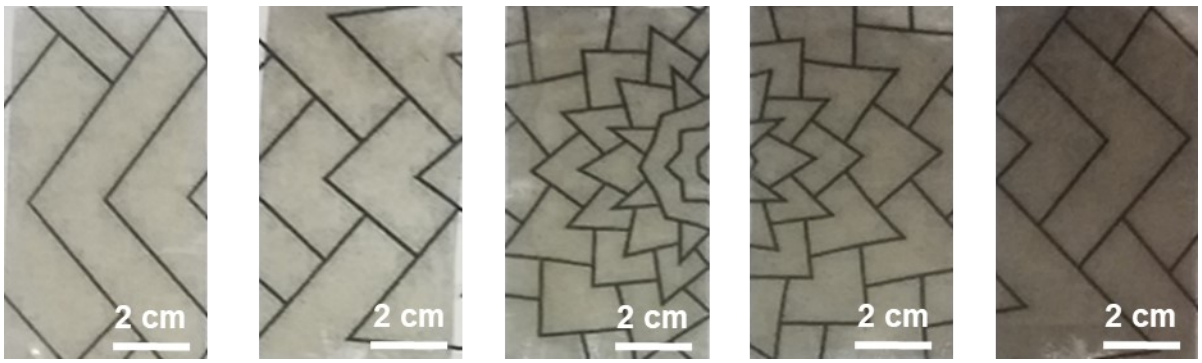

Fig. S11. Photographs of the 3, 5, 8, 10 and 15 layers of 8 wt.% $W_{18}O_{49}$ NW/rGO composite deposited on Ag/$W_{18}O_{49}$ NW PET substrate.

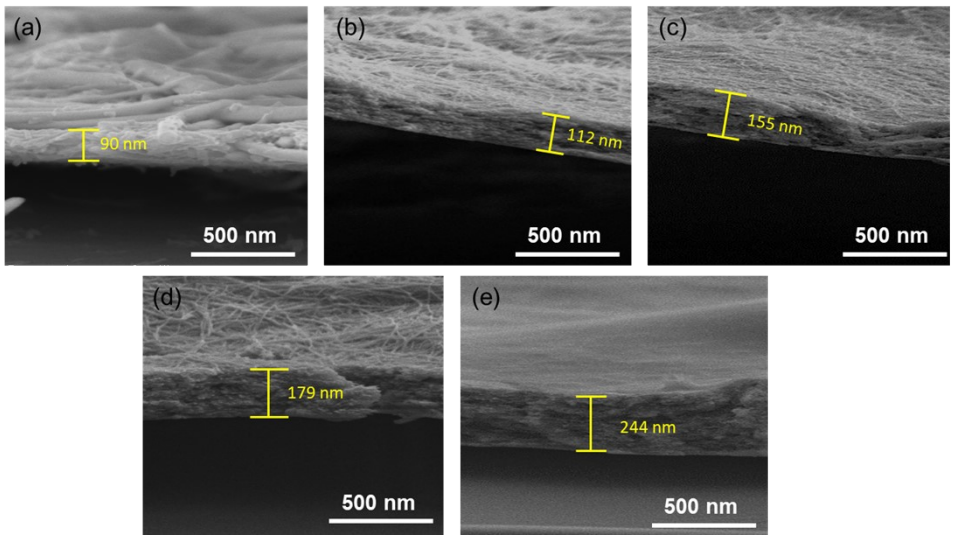

Fig. S12. Cross-Sectional SEM images of 3, 5, 8, 10 and 15 layers $W_{18}O_{49}$ NW/rGO composite film.

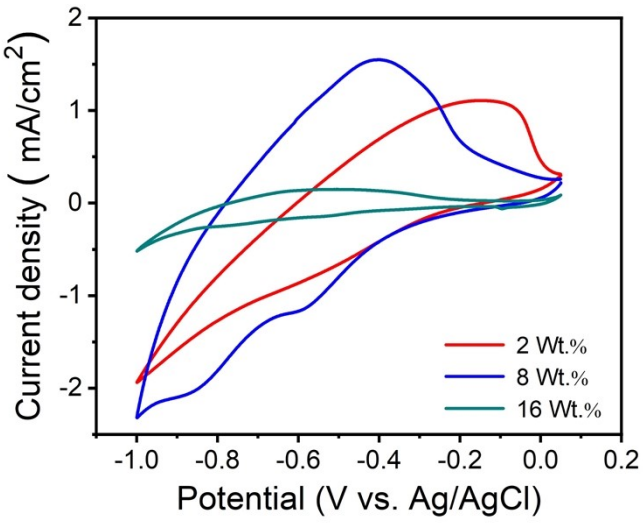

Fig. S13. CV plots of 15 L $W_{18}O_{49}$NW/rGO composite film electrode containing different amount of rGO at 20 mV/s.

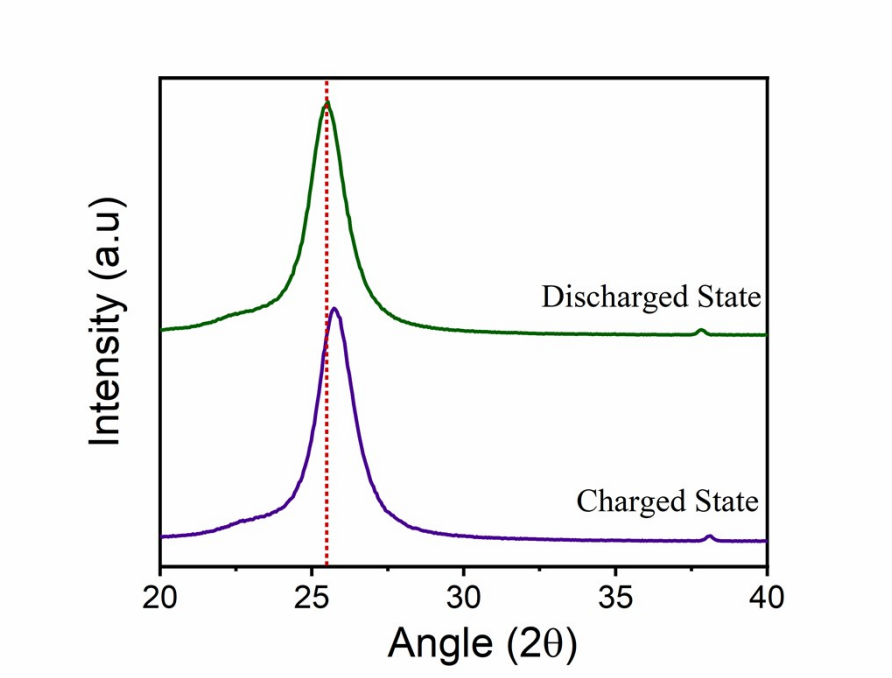

Fig. S14. XRD spectra of hybrid electrode at charge and discharge state.

Table S1: Comparison of transmittance, areal capacitance of reported literature with fabricated hybrid electrode.

Material	Transparency %	Electrolyte	capacitance mF/cm^2	Measuring current	Ref
Ag NWs)/PEDOT: PSS with a $Ni(OH)_2$-PEIE interlayer	86	LiCl	4.43	-	[1]
WO_3 electrode	76	KOH	2.57	1 mA/cm^2	[2]
MnO_2@Ni electrode	84	Na_2SO_4	80.75	5 mV/s	[3]
Island like MnO_2 Arrays	68.7	Na_2SO_4	13.44	100 mV/s	[4]
MnO_2/Au nanofibers electrode	71	Na_2SO_4	4.03	mA cm^{-2}	[5]
Ag-Au alloy	90.1	H_2SO_4	12.1	0.1 mA/cm^2	[6]
core-shell Cu@Ni@NiCoS nanofibers	76.83	Ni:CoS	0.00694	0.066 mA/cm^2	[7]
MXene (Ti_3C_2Tx) Films	86	Na_2SO_4	3.4	5 mV/s	[8]
$Cu_3(HHTP)_2$ (HHTP = 2,3,6,7,10,11-hexahydroxytriphenylene) film	82.2	KCl	1.7	30 µA/cm^2	[9]
poly(5-formylindole)/WO_3	60	H_2SO_4-PVA	34.1	0.1 mA/cm^2	[10]
Our work	72	$AlCl_3$	88	2 mA/cm^2	

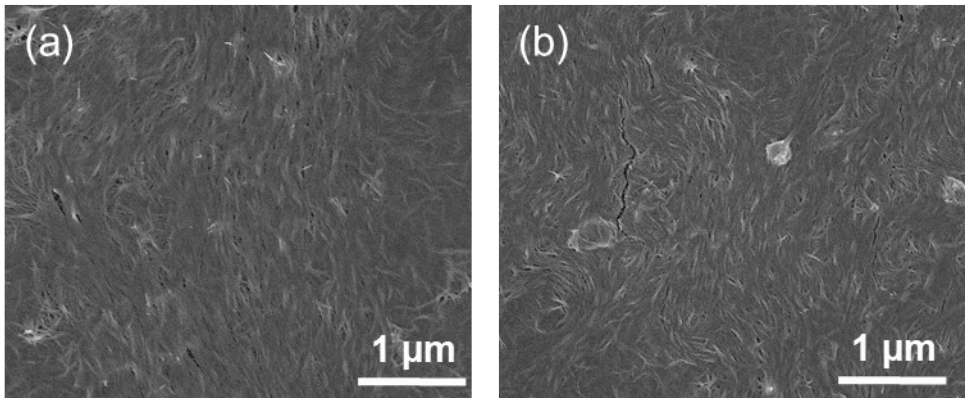

Fig. S15. (a, b) SEM image hybrid electrode before and after charging process.

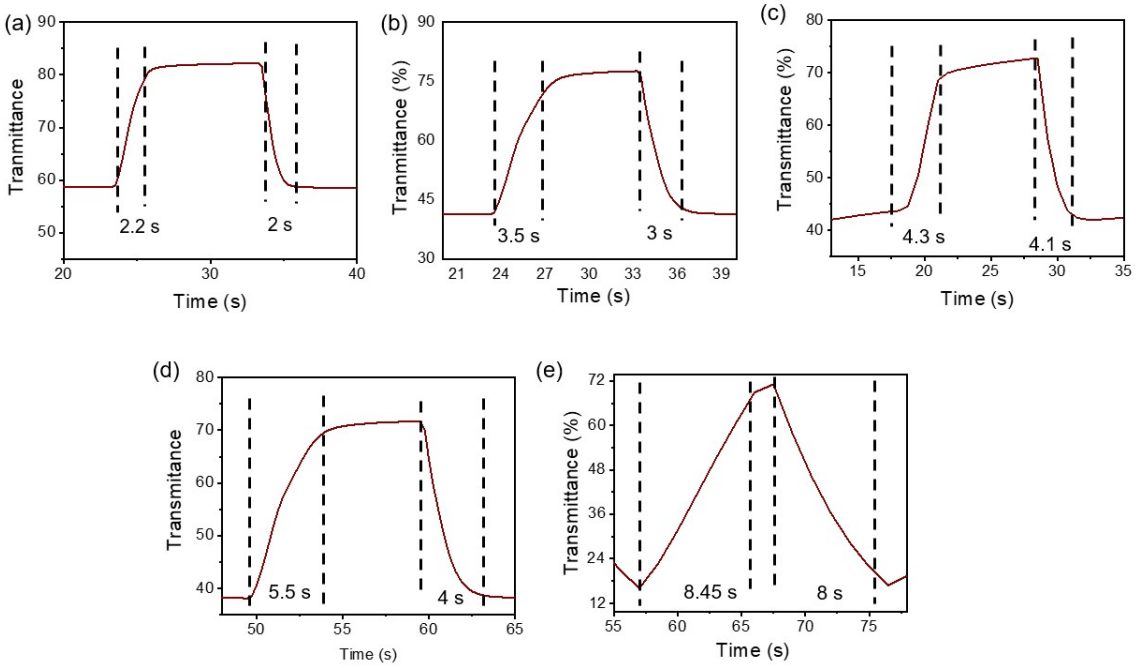

Fig. S16. Bleaching and coloration time of the $W_{18}O_{49}$NW/rGO composite film with different layers of $W_{18}O_{49}$ NW/rGO composite. (a) Three layers; (b) Five layers; (c) Eight layers; (d) Ten layers; and (e) Fifteen layers of $W_{18}O_{49}$NW/rGO composite.

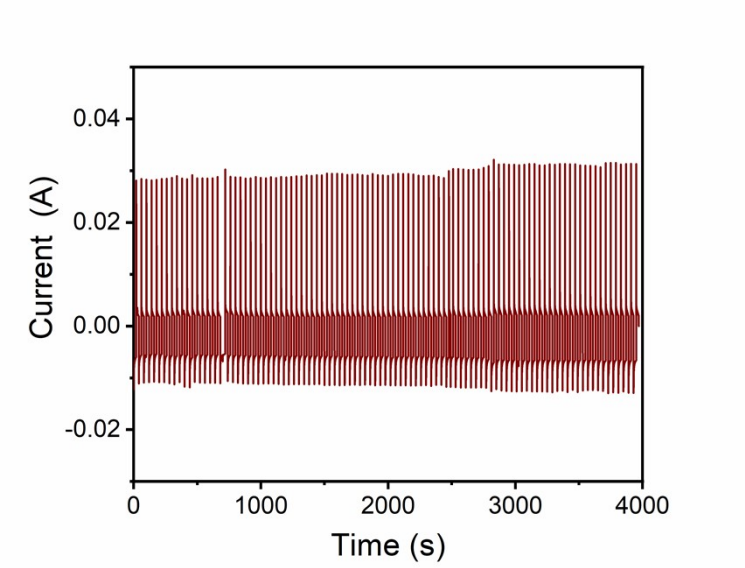

Fig. S17. Electrochromic switching of 15 layers $W_{18}O_{49}$ NW/rGO composite electrode for 4000 s.

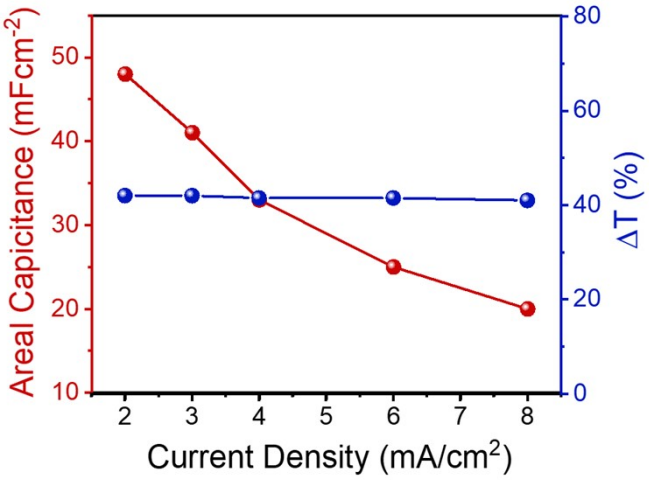

Fig. S18. Areal capacitance and optical modulation of the 15-layers 2 wt.% $W_{18}O_{49}$ NW/rGO composite films supercapacitor device as a function of the current density

Table S2: Comparison of energy density and power density of reported literature with fabricated supercapacitor device.

Active material	Power density (mW cm^{-2})	Energy density (μWh cm^{-2})	Ref
Cu@Ni@NiCoS	0.0111	0.49	7
	0.0152	0.34	
	0.0191	0.27	
	0.0228	0.21	
	0.0261	0.17	
	0.0296	0.15	
	0.031	0.14	
AgNW/$Ni(OH)_2$PEIE/PEDOT:PSS	0.0032	0.074	1
	0.004	0.072	
	0.006	0.069	
	0.012	0.059	
	0.020	0.05	
$Co(OH)_2$/AgNWs	0.0288	0.04	11
	0.0435	0.0375	
	0.0573	0.035	
	0.0706	0.0335	
	0.0831	0.03	
	0.0945	0.02665	
	0.0106	0.02625	
MnO_2@AuNFs	0.004	0.143	12
	0.008	0.101	
	0.012	0.078	
	0.016	0.066	
	0.020	0.054	
$Ti_3C_2T_x$	0.0006	0.049	13
	0.0012	0.034	
	0.0025	0.025	
	0.0051	0.02	
	0.0109	0.018	
$W_{18}O_{49}$/rGO composite film	0.391	5.2	**This work**
	0.461	4.61	
	0.53	3.71	
	0.936	2.81	
	2.21	2.25	

1. R. T. Ginting, M. M. Ovhal and J.-W. Kang, *Nano Energy*, 2018, **53**, 650-657.
2. K.-W. Kim, T. Y. Yun, S.-H. You, X. Tang, J. Lee, Y. Seo, Y.-T. Kim, S. H. Kim, H. C. Moon and J. K. Kim, *NPG Asia Mater.*, 2020, **12**.
3. Y.-H. Liu, J.-L. Xu, X. Gao, Y.-L. Sun, J.-J. Lv, S. Shen, L.-S. Chen and S.-D. Wang, *Energy Environ. Sci.*, 2017, **10**, 2534-2543.
4. Y. Wang, W. Zhou, Q. Kang, J. Chen, Y. Li, X. Feng, D. Wang, Y. Ma and W. Huang, *ACS Appl. Mater. Interfaces*, 2018, **10**, 27001-27008.
5. Y. Lee, S. Chae, H. Park, J. Kim and S.-H. Jeong, *Chem.Engineer.J*, 2020, **382**.
6. H. Zhang, Y. Tian, S. Wang, Y. Huang, J. Wen, C. Hang, Z. Zheng and C. Wang, *Chem.Engineer.J*, 2020, **399**, 125075.
7. B. S. Soram, I. S. Thangjam, J. Y. Dai, T. Kshetri, N. H. Kim and J. H. Lee, *Chem.Engineer.J*, 2020, **395**.
8. D. Wen, X. Wang, L. Liu, C. Hu, C. Sun, Y. R. Wu, Y. L. Zhao, J. X. Zhang, X. D. Liu and G. B. Ying, *ACS Appl. Mater. Interfaces*, 2021, **13**, 17766-17780.
9. W. W. Zhao, T. T. Chen, W. K. Wang, S. H. Bi, M. Y. Jiang, K. Y. Zhang, S. J. Liu, W. Huang and Q. Zhao, *Adv.Mater.Interfaces*, 2021, **8**.
10. Q. Guo, X. Zhao, Z. Li, D. Wang and G. Nie, *Chem.Engineer.J*, 2020, **384**.
11. H. Sheng, X. Zhang, Y. Ma, P. Wang, J. Zhou, Q. Su, W. Lan, E. Xie and C. J. Zhang, *ACS Appl. Mater. Interfaces*, 2019, **11**, 8992-9001.
12. S. B. Singh, T. I. Singh, N. H. Kim and J. H. Lee, *J.Mater.Chem.A*, 2019, **7**, 10672-10683.
13. C. Zhang, B. Anasori, A. Seral-Ascaso, S.-H. Park, N. McEvoy, A. Shmeliov, G. S. Duesberg, J. N. Coleman, Y. Gogotsi and V. Nicolosi, *Adv.Mater.*, 2017, **29**.